



Influence of augmentation of biochar during anaerobic co-digestion of *Chlorella vulgaris* and cellulose

Jessica Quintana-Najera^a, A. John Blacker^{a,b}, Louise A. Fletcher^c, Andrew B. Ross^{a,*}

^a School of Chemical and Process Engineering, University of Leeds, LS2 9JT Leeds, UK

^b Institute of Process Research and Development, School of Chemistry, University of Leeds, LS2 9JT Leeds, UK

^c School of Civil Engineering, University of Leeds, LS2 9JT Leeds, UK

HIGHLIGHTS

- Biochar addition improved biomethane yield particularly at less favourable ISR 0.5–0.9.
- Biochar provided a buffering effect at lower ISR and C/N ratio.
- Factorial regression model provided optimal anaerobic co-digestion conditions.
- Biochar effect is highly dependent on the digestion conditions.

ARTICLE INFO

Keywords:

Anaerobic co-digestion
Biochar
Pyrolysis
Biomethane optimization
Microalgae

ABSTRACT

The anaerobic co-digestion (AcoD) of microalgae is a prospective option for generating biomethane from renewable sources. This study investigates the effects of inoculum-to-substrate ratio (ISR), C/N ratio and biochar (BC) load on the AcoD of *Chlorella vulgaris* and cellulose. An initial augmentation of BC at ISR 0.5–0.9 and C/N ratio 10–30 offered a pH buffering effect and resulted in biomethane yields of 233–241 mL CH₄/g VS, corresponding to 1.8–4.6 times the controls. BC addition ameliorated significantly AcoD, supporting the digestate stability at less favourable conditions. The effect of the process variables was further studied with a 2³ factorial design and response optimisation. Under the design conditions, the variables had less influence over methane production. Higher ISRs and C/N ratios favoured AcoD, whereas increasing amounts of BC reduced biomethane yield but enhanced production rate. The factorial design highlighted the importance of BC-load on AcoD, establishing an optimum of 0.58 % (w/v).

1. Introduction

Biomethane is a valuable option towards a sustainable and low-emissions future due to its compatibility with gas infrastructure. Currently, biomethane represents only 0.1% of natural gas demand, however, recent policy changes towards decarbonising transport are supporting its injection into natural gas grids. Many countries like Germany, Netherlands, United Kingdom, Brazil and the USA are supporting the introduction of biomethane into the transport sector. Since 2010, the installed biogas power generation capacity has been growing 4 % annually, however, this future development is highly dependent on feedstock availability (IEA, 2020).

Microalgae is an attractive feedstock for biofuel production due to their highly productive growth, and photosynthetic solar efficiency that

doubles the terrestrial plants. Among the advantages of microalgae is the utilisation of land areas unsuitable for food production, utilise carbon dioxide emissions, resulting in lower land-use footprint and providing carbon-neutral biofuels. There are different types of microalgae, including the ‘weed’ green species *Chlorella vulgaris*, which is considered a rich biomass source, with a low content of toxic compounds, rapid growth rate and high protein content (Chronakis and Madsen, 2011). However, the demanding nutrient requirements and recalcitrant cell wall of *C. vulgaris* hinders its biodegradability (BD) (Ward et al., 2014). Increasing the BD of microalgae can be achieved by physical–chemical pre-treatments, however, this is often uneconomically or energetically unjustified.

Coupling microalgae cultivation with anaerobic digestion (AD) is suggested to overcome some of the inherent limitations (Ward et al.,

* Corresponding author.

E-mail address: a.b.ross@leeds.ac.uk (A.B. Ross).

<https://doi.org/10.1016/j.biortech.2021.126086>

Received 4 August 2021; Received in revised form 30 September 2021; Accepted 1 October 2021

Available online 6 October 2021

0960-8524/© 2021 The Authors. Published by Elsevier Ltd. This is an open access article under the CC BY license (<http://creativecommons.org/licenses/by/4.0/>).

2014). A circular process where nutrients from the anaerobic sludge are recovered for microalgae growth could improve economic and energy efficiency. Whereas the anaerobic co-digestion (AcoD) of microalgae with another carbon-rich substrate could improve the BD (Wang et al., 2013). AcoD of complex substrates offers several technological, ecological and economic advantages. A properly balanced co-digestion can provide synergistic effects, improve the process stability, methane yield, kinetic parameters, and in consequence the economic viability of biomethane (Li et al., 2017).

AcoD of an N-rich and a C-rich substrate at an adequate C/N ratio can supply the N requirements for microorganisms and alleviate pH changes due to acid products. The co-digestion of *C. vulgaris* with a reference substrate with known degradability, in this case cellulose, allows the effect of biochar augmentation on C/N ratios to be investigated and allows optimum C/N ratio to be controlled. Reports of improved methane yields of *C. vulgaris* in co-digestion with C-rich biomass have been attributed to adequate C/N ratios (Zhang et al., 2019). Adequate C/N ratios are often found at 15–30, although the optimum value is highly dependent on the feedstock (Yao et al., 2017). For instance, the optimal C/N ratio varied for crops 20 (Piątek et al., 2016), corn stover 25 (Yao et al., 2017), algae 25–30 (Bohutskyi et al., 2018), and microalgae 20–25 (Yen and Brune, 2007).

Other approaches could complement AcoD, such as implementing optimal inoculum to substrate ratio (ISR) and AD amendment by adding adsorbent carbon materials. The inoculation influences the initial activity and performance of the digester. Hence, ISR is an essential operating condition that needs to be evaluated for optimising digestion (De la Rubia et al., 2018). The implementation of optimum ISR helps maintain the digester stability, avoid the accumulation of volatile fatty acids (VFAs), and reduce the necessity of nutrient media supplementation while obtaining better methane yields (Okoro-Shekwaga et al., 2020).

The addition of biochar (BC) in AD is reported to enhance methane production rate and yields (Quintana-Najera et al., 2021), mitigate ammonium inhibition (Mumme et al., 2014), promote methanogenic metabolism, reduce the lag phase (Shanmugam et al., 2018), and improve the syntrophic oxidation of VFAs (Paritosh and Vivekanand, 2019). The positive effect of BC has been attributed to its advantageous physicochemical properties. A developed porosity provides a large surface area (SA) for the interaction and immobilisation of the cells. While the surface oxygenated functional groups (OFGs) are reported to serve as anchoring and interaction sites for biomolecules that facilitate direct interspecies electron transfer (DIET) interactions between microorganisms (Zhao et al., 2015). Nonetheless, not all BCs have the desired properties or positive effects on AD. Thus, the possibility to tailor the BC properties to fulfil desired characteristics by controlling the pyrolysis conditions strengthens its applications and versatility (Lee et al., 2017).

Although many studies have reported AcoD for enhancing methane yields, the simultaneous addition of BC could provide another promising approach. Therefore, the current study was undertaken to establish the potential of BC for enhancing methane generation during the AcoD of *C. vulgaris* and cellulose and to identify the optimal digestion conditions. The first aim was to investigate the effect of BC at different C/N ratios and ISR on methane yields and kinetic parameters. The second aim was to use a factorial design 2^3 for identifying the optimum BC load and ISR during the AcoD of *C. vulgaris* and cellulose at different C/N ratios.

2. Materials and methods

2.1. Inoculum, substrate and biochar

Anaerobic sludge collected from the mesophilic wastewater treatment plant Esholt in Bradford, United Kingdom was collected and stored at 4 °C. Before use, the inoculum was homogenised by passing it through a mesh (1 mm). The total solids (TS) and volatile solids (VS) were quantified gravimetrically (APHA, 2005). The substrates used were the microalgae *C. vulgaris* and cellulose. Autotrophic *C. vulgaris* was

produced and dried in China and cracked in a ball mill at the University of Leeds. The composition of *C. vulgaris* was analysed as: i) biochemical (protein 40.5 %, lipids 15.6 %, and carbohydrates 36 %); ii) proximate (volatile matter 77.1 %, fixed carbon 14.3 % and ash 8.6 %); iii) ultimate (C 54.6, H 8.1, N 9.3, O 19.5 %). Proximate analysis was determined using a thermogravimetric analyser (TGA) Mettler Toledo (TGA/DSC 1). For elemental analysis, an automatic CHNS Thermo Instruments Flash (EA 1112 Series) was employed with values expressed as a percentage of total dry weight, with total oxygen (O) determined by difference. Cellulose was selected as the C-rich substrate because as a model substrate it facilitated the C/N ratio calculation, and is regarded as a reference for other agricultural feedstocks since it often represents their primary component. Oak wood BC was produced at 450 °C at commercial pyrolysis operated by Proinso (Spain), its physicochemical properties were characterised elsewhere (Quintana-Najera et al., 2021).

2.2. Biochemical methane potential

Biochemical methane potential (BMP) measurement was performed with the Automatic Methane Potential Test System (AMPTS II) (Bioprocess Control, Sweden) and calculated as expressed in Eq. (1). The AcoD experiments were performed in 500 mL reactors with a working space of 400 mL. After filling the reactors with the desired conditions, they were flushed with nitrogen for establishing anaerobic conditions. The reactors were incubated at 37 °C for 30 days and automatically stirred for 60 s every 10 min.

$$BMP = \frac{\text{Volume } CH_4 \text{ from sample (mL)} - \text{Volume } CH_4 \text{ from blank (mL)}}{\text{g VS of substrate fed in digester}} \quad (1)$$

2.3. Anaerobic co-digestion of microalgae and cellulose

The conditions for the first AcoD experiments consisted of inoculum 5 g VS/L, BC load 0 and 3 % (w/v), cellulose 5 g VS/L and variable amounts of *C. vulgaris* for achieving C/N ratios of 10, 20 and 30, respectively. The necessary amount of *C. vulgaris* was calculated based on the chemical composition of both substrates. The increasing amount of *C. vulgaris* for obtaining C/N ratios of 10, 20 and 30 reduced the ISRs to 0.5, 0.8 and 0.9, respectively. Controls consisting of inoculum and substrate at each C/N ratio and ISR, without BC, alongside a blank consisting only of inoculum to account for residual methane emissions were performed in parallel. The treatments with BC at each C/N ratio were performed by triplicate, whereas the controls and blank were performed by duplicate. The C/N ratios ranged between optimum values (20–30) and sub-optimal (10). The objective of this was to establish the potential of the BC in ameliorating critical processing conditions during the AcoD of microalgae and cellulose.

2.4. Theoretical biochemical methane potential

The theoretical BMP (BMP_{th}) of a substrate can be estimated from its chemical composition according to the Boyls equation (Eq. (2)). This equation assumes a substrate breakdown efficiency of 100 % and considers only the products CH_4 and CO_2 . The ash content was subtracted from the calculation and only the biodegradable fraction was considered, hence the BMP_{th} is expressed as mL CH_4 /g VS. Eq. (2) is calculated at STP conditions (273 K, 1 atm), where c, h, o and n represent the molar fractions of C, H, O and N, respectively (Aragón-Briceno et al., 2020; Buswell and Mueller, 1952). The values for *C. vulgaris* ($BMP_{th,a}$) and cellulose ($BMP_{th,b}$) were further used to establish the BMP_{th} of their combination according to Eq. (3). C_a and C_b are their corresponding mass fraction used at the different C/N ratios.

$$BMP_{th} = \frac{22400 * (\frac{c}{2} + \frac{h}{8} - \frac{o}{4} - \frac{3n}{8})}{12c + h + 16o + 14n} \quad (2)$$

$$BMP_{th} = (BMP_{th,a} * C_a) + (BMP_{th,b} * C_b) \quad (3)$$

2.5. Anaerobic biodegradability

The anaerobic BD of methane for each treatment considered the combination of substrates at a given C/N ratio. BD was calculated from the final experimental BMP and the BMP_{Th} according to Eq. (4) (Aragón-Briceno et al., 2020).

$$BD(\%) = \frac{BMP}{BMP_{Th}} * 100 \quad (4)$$

2.6. Kinetic analysis

The experimental BMP values were fitted to the modified Gompertz model (Eq. (5)) according to Zwietering et al. (1990).

$$BMP(t) = BMP_{max} * \exp \left\{ - \exp \left[\frac{\mu_m * e}{BMP_{max}} (\lambda - t) + 1 \right] \right\} \quad (5)$$

where; $BMP(t)$ = Cumulative methane yield (mL CH_4/g VS) at time t (day), BMP_{max} = Maximum methane yield (mL CH_4/g VS), μ_m = Methane production rate (mL CH_4/g VS·day), λ = Lag phase (days), $e = \exp(1)$.

2.7. Factorial design 2^3

To determine the optimum processing conditions for the AcoD of *C. vulgaris* and cellulose, a full factorial 2^3 experimental design was performed. The study comprised three independent factors at two levels, C/N ratio (7 and 25), ISR (1 and 2) and BC load (0 and 3 %) with 3 replicates and 3 centre points (C/N 16, ISR 1.5 and BC load 1.5 %). The inoculum was fixed at 10 g VS/L, whereas the amount of substrate added ranged from 5 to 10 g VS/L for achieving the corresponding ISR. The amount of *C. vulgaris* and cellulose added for each C/N ratio and ISR were calculated based on their chemical composition. For achieving the C/N ratio of 7, 16 and 25, the ratio of *C. vulgaris* to cellulose were 0.8:0.2, 0.3:0.7 and 0.2:0.8, respectively. A factorial regression model was used for analysing biomethane production (Montgomery, 2013). The desirability (D) function was used for optimising the AcoD conditions. The main objective of this experiment was to investigate and optimise the effect of BC load and ISR under variable C/N ratios.

2.8. Analytical methods

The amount of VFAs accumulated at the end of the AcoD was measured by gas chromatography. An Agilent 7890A gas chromatograph, a DB-FFAP column (30 m × 0.32 mm, film thickness of 0.5 μm) and a flame ionisation detector (FID) at 200 °C with nitrogen as make-up gas was used. An autosampler injected 10 μL of the sample at a 5:1 split ratio. The inlet port operated at 150 °C with helium at 10 mL/min as a carrier gas. The column oven started at 60 °C for 4 min, then increased to 140 °C with a ramp of 10 °C/min, and finally raised to 200 °C with a ramp of 40 °C/min and held for 5 min. A volatile acid standard mix (Supelco) and alcohols made from high purity single reagents were used as comparative standards. Data was acquired with ChemStation software. Ammonia can be found in the digester in the form of free or non-ionised ammonia (NH_3) and ionised ammonium (NH_4^+). Ammonia was detected by a spectrophotometer (DR 3900, HACH) using the LCK305 ammonium cuvette test 1.0–12.0 mg/L NH_4-N/NH_3-N test based on the indophenol blue method and according to ISO 7150–1 and DIN 38,406 E5-1 water quality standards. Total ammonia nitrogen (TAN) is expressed as the sum of NH_4-N and NH_3-N . The solid fraction decanted at the end of the digestion was oven-dried and evaluated by CHNOS elemental analysis.

2.9. Statistical analysis

The SPSS Statistics 26 software was used for most statistical analyses and to calculate the Gompertz kinetic parameters. While Minitab 27 software was used for creating the factorial design and analysing the response variables, models and optimisation. Comparison of the effect of the factors C/N ratio, ISR and BC load over the data was performed by analysis of variance (ANOVA) and linear regression at a confidence level of $p < 0.05$.

3. Results and discussion

3.1. Exploratory anaerobic co-digestion experiments

3.1.1. Experimental biochemical methane potential

Fig. 1 shows the cumulative BMP with and without the addition of BC during the AcoD of cellulose and *C. vulgaris* at 10–30C/N ratios and ISR 0.5–0.9. All systems started generating methane since day one, although the controls rapidly reached maximum production and steady-state. Conversely, the BC systems showed an initial plateau, followed by second exponential and stationary phases.

For the controls, reducing the C/N ratio and ISR resulted in lower BMP yields due to less favourable conditions. Nonetheless, the C/N ratio and ISR showed no statistically significant effect over the final BMP_{Exp} yield ($p > 0.05$). The detrimental impact of reducing the C/N below the optimal could be attributed to ammonia accumulation and toxicity (Bohutskyi et al., 2018). Also to the low ISR range employed, since ISR below 0.8 is reported to facilitate the proliferation of acidogens and acetogens and inhibition of methanogens (Moset et al., 2015). The BMP was similar for the BC systems at C/N ratios of 10, 20 and 30, achieving final yields of 233, 239 and 241 mL CH_4/g VS, respectively. These values corresponded to an enhance of 4.6, 2.6 and 1.8 times their control, respectively. The dramatic improvement of BMP yields due to the BC addition suggested that BC could have ameliorated the co-digestion of microalgae and cellulose, particularly at less favourable conditions.

3.1.2. Kinetic modelling

Table 1 shows the kinetic parameters obtained by fitting the experimental BMP to the modified Gompertz model. BMP_{max} at the C/N ratios of 10, 20 and 30 was 82, 66 and 51 % higher for the systems augmented with BC in comparison to their control, respectively. The controls quickly reached the steady-state, which was reflected in their higher μ_m in comparison to the BC systems. Both variables BMP_{max} and μ_m had a

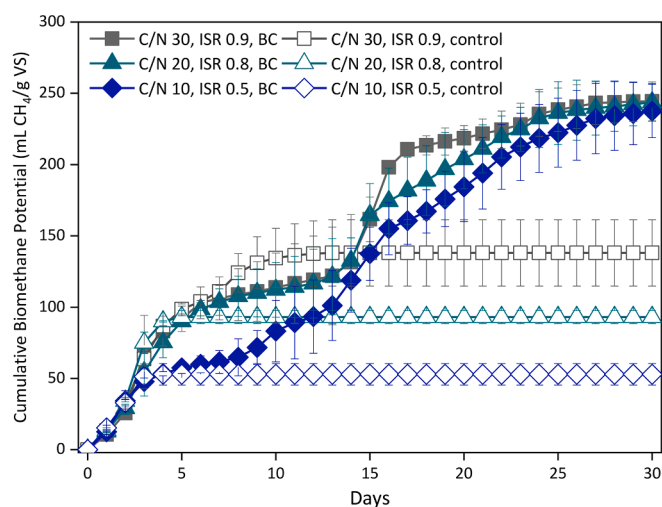


Fig. 1. Effect of biochar augmentation on the biochemical methane potential for the exploratory anaerobic co-digestion of cellulose and *Chlorella vulgaris* at C/N ratios 10–30 and ISRs 0.5–0.9.

Table 1

Biomethane experimental yield and kinetic parameters obtained with the modified Gompertz model for anaerobic co-digestion of cellulose and *Chlorella vulgaris* with the addition of oak wood biochar.

Systems	Experimental data			Modified Gompertz model			
	BMP _{Th} (mL CH ₄ /g VS)	BMP _{Exp} (mL CH ₄ /g VS)	BD(%)	BMP _{max} (mL CH ₄ /g VS)	μ _m (mL CH ₄ /g VS-day)	λ(days)	R ²
C/N 10, ISR 0.5, BC	506.5	232.7	46.0	278.6	9.5	1.0	0.987
C/N 10, ISR 0.5, control	506.5	50.8	10.0	50.9	23.6	0.4	0.993
C/N 20, ISR 0.8, BC	459.6	239.1	52.0	270.2	10.0	0.0	0.972
C/N 20, ISR 0.8, control	459.6	91.2	19.8	91.4	39.5	1.0	0.993
C/N 30, ISR 0.9, BC	444.4	241.2	54.3	275.5	12.4	0.0	0.975
C/N 30, ISR 0.9, control	444.4	136.2	30.7	136.2	22.7	0.5	0.994

BMP_{Exp} maximum experimental methane yield, BD biodegradability; BMP_{max} maximum methane yield; μ_m methane production yield; λ duration of lag phase; BC addition of 3 % (w/v),

statistically significant difference with the BC addition ($p < 0.05$). However, neither the C/N ratio nor ISR showed significance over these kinetic parameters ($p > 0.05$). Increasing the C/N ratio and ISR reduced the period of the lag phase, although not significantly ($p > 0.05$). BC addition was the factor with the highest influence over the AD kinetic parameters, suggesting that BC positively influenced AcoD performance.

3.1.3. Biodegradability

The BMP_{Th} for *C. vulgaris* (607 mL CH₄/g VS) is considerably higher than cellulose (415 mL CH₄/g VS) due to the high content of protein and lipids of the former (Bohutskyi et al., 2018). Hence, the differences in BMP_{Th} were a consequence of the amount of microalgae added for achieving each C/N ratio. The BD with the addition of BC and non-BC controls at the three C/N ratios ranged at 46–54 % and 10–31 %, respectively (Table 1). The achieved BD values were far from the theoretical maximum which is partially attributed to the limiting BD of microalgae due to its thick and recalcitrant cell wall. Even though *C. vulgaris* was physically pre-treated by ball-milled cracking. The BD could only improve up to a certain extent since it has been stated that a fraction of undigested microalgae usually remains intact throughout the AD process (Ward et al., 2014). Furthermore, the BDs were generally lower in comparison to previous BMP tests where the same concentration of cellulose was added as mono-substrate (BD 64–70 %) (Quintana-Najera et al., 2021). Hence, an inhibitory effect originated principally by *C. vulgaris* and low ISR could have hindered the BD and BMP values, less drastically for the systems supplemented with BC than the controls and directly correlated to the reduction of C/N ratio.

3.1.4. Volatile fatty acids and pH

Fig. 2a shows the VFAs accumulated at the end of the AcoD experiments. The systems that produced lower amounts of BMP also resulted in higher VFAs accumulation. The controls (C/N 20, ISR 0.8) and (C/N 30, ISR 0.9) showed a similar accumulation of VFAs, whereas the control (C/N 10, ISR 0.5) reached 1239 mg total VFAs/L. On the other hand, the BC systems at C/N ratios of 10 and 30 exhibited negligible VFAs. Although the system (C/N 20, ISR 0.8, BC) accumulated 363 mL total VFAs/L. Nevertheless, no system reached toxic levels since acetic inhibition on methanogens is reported to take place at concentrations above 1619 mg/mL (Xiao et al., 2013).

Fig. 2b shows the pH measured at the beginning and the end of the AcoD process. All systems started with a similar pH (7.4–7.7), which by the end of the fermentation suffered negligible variations on the reactors supplemented with BC. The controls, on the other hand, suffered a drastic pH reduction (pH 5.3–5) that intensified at lower C/N ratios and ISR. The changes in pH agree with the BMP_{Exp} values, as those systems whose pH suffered more variation also produced less BMP. The latter suggests that the oak wood BC here used could have provided a buffering effect given its alkaline nature (pH 9.9). Similarly, there are reports of BC having a positive buffering role in AD (Paritosh and Vivekanand, 2019; Wang et al., 2018). A digester with adequate alkalinity would stabilise the AD process from variations of VFAs and pH. However, if the alkalinity is insufficient, the digester would undergo acidosis and the

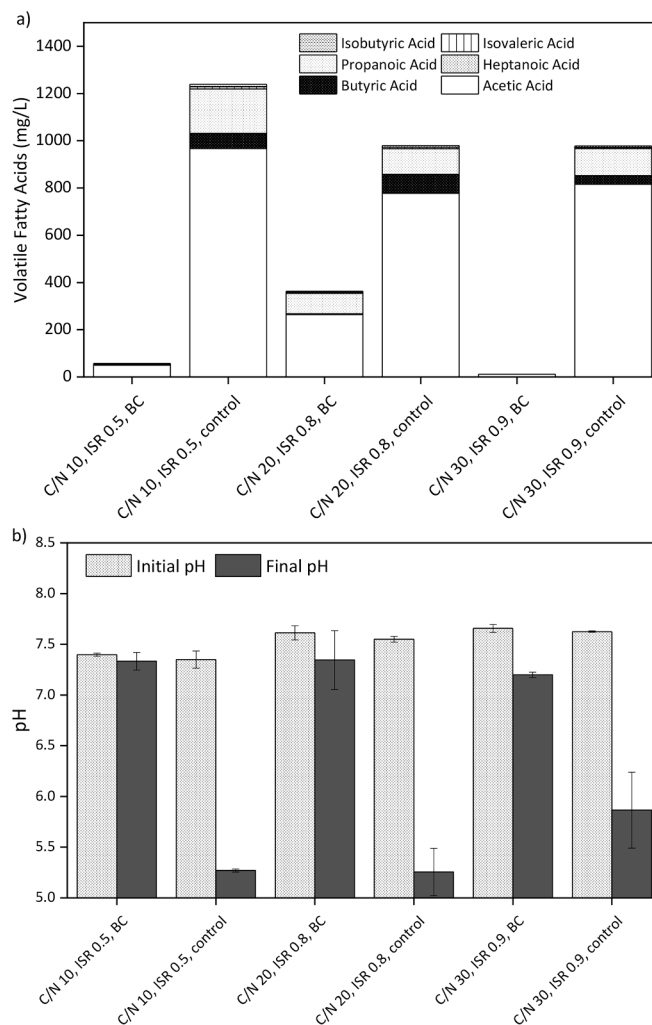


Fig. 2. Effect of biochar augmentation on the anaerobic co-digestion of cellulose and *Chlorella vulgaris* at C/N ratios 10–30 and ISRs 0.5–0.9. a) Accumulated volatile fatty acids; b) pH.

methane production would cease (Sterling et al., 2001).

3.1.5. Biochar in anaerobic co-digestion

BMPs and BD were hindered with the increasing addition of *C. vulgaris* (C/N reduction) and in consequence the increase of N-content. This behaviour was drastically observed for the non-BC controls, whereas it was considerably milder for the BC systems. The better BMP performance in the presence of BC could be attributed to the beneficial properties of BC, such as alkalinity, conductivity, SA and possible role as a facilitator of syntrophic metabolism via DIET interactions (Klöpffel

et al., 2014; Quintana-Najera et al., 2021). The characterisation of the oak wood BC produced at 450 °C, used for this work was detailed in a previous publication. The BC showed a developed SA of 221 m²/g and pore volume (PV) of 0.09 m³/g and large availability of OFGs (Quintana-Najera et al., 2021). The SA and PV could provide a suitable environment for interaction and/or adsorption of molecules between the different microorganisms. While the OFGs, often dominated by quinone/hydroquinone functionalities, could have been responsible for redox buffering capacity and facilitators of DIET interactions (Klöpffel et al., 2014). Therefore, this experiment demonstrated that BC addition could fulfil the necessity of an alkaline source, avoid drastic changes in pH and maintain the stability of the AD process under the conditions here studied. However, it is desirable to establish the best blend ratios for the substrates and inoculum for achieving positive synergisms, nutrient balance, avoid inhibition, and optimise methane productivity (Mata-Alvarez et al., 2011). Hence, the following section evaluates the optimum conditions for the AcoD of microalgae and cellulose to obtain a better BMP performance.

3.2. Factorial design

3.2.1. Experimental biochemical methane potential

Fig. 3 shows the average BMP produced by each condition of the factorial design for the AcoD of *C. vulgaris* and cellulose. All systems started producing methane since day one exhibiting a quick exponential phase while reaching the steady-state by the 10th day of digestion. The final BMP yields differed by up to 17 % among the conditions since they were found in a range of 247–299 mL CH₄/g VS (Table 2). The highest BMP yield was obtained by the system (C/N 25, ISR 1.0, BC load 0 %), while the lowest yield was obtained at (C/N 7, ISR 1.0, BC load 3.0 %). BMP yields were enhanced by increasing the C/N ratios due to more favourable conditions. Increasing the BC load appeared to reduce BMP yields, whereas ISR showed no consistent trend.

The final BMP yields assuming additive behaviour obtained from the mono-AD of *C. vulgaris* and cellulose with and without BC addition is compared to the actual BMP data observed during co-digestion and is shown in the supplementary data. The additive BMP for the combination of cellulose and *C. vulgaris* at each C/N ratio was calculated based on the fraction of each substrate and the final BMP obtained from their mono digestion (supplementary material). This allowed a comparison of any synergy during co-digestion with or without the addition of BC.

A synergistic increase in BMP was observed during co-digestion of the two substrates in comparison to predicted additive behaviour based on mono-digestion. This improvement was observed at most conditions

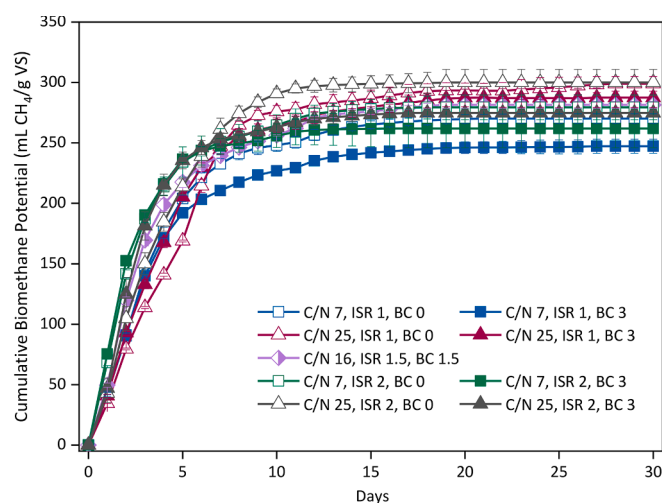


Fig. 3. Biochemical methane potential for the anaerobic co-digestion of cellulose and *C. vulgaris* for the factorial design 2³ conditions.

of the DoE, particularly at lower ISR and C/N ratios (supplementary material). Increasing the ISR improved the mono digestion of the two substrates, in agreement with other reports (Zhang et al., 2019). However, this was also accompanied by an increase in BMP during co-digestion.

The amount of synergistic increase in BMP during co-digestion was reduced when adding 3 wt% BC, however when optimum BC loading was added (0.6 wt%), the synergistic increase was higher than co-digestion without BC. This illustrates the importance of BC loading as well as the benefits of co-digestion of an additional carbon source for the digestion of *C. vulgaris*.

3.2.2. Kinetic modelling

Table 2 shows the kinetic parameters obtained with the modified Gompertz model. The values of BMP_{max} were gradually improved as the C/N ratio increased and the BC load reduced. The period of lag phase was almost negligible for all systems, while μ_m showed the greatest variation. The highest μ_m of 70.2 and 66.2 mL CH₄/g VS-d, were obtained at the conditions (C/N 7, ISR 2.0, BC 3.0) and (C/N 25, ISR 2.0, BC 3.0), respectively. The rest of the systems exhibited values of 40–55 mL CH₄/g VS-d, corresponding to 16–39 % lower μ_m than the best performers. The effect of the C/N ratio showed no evident trend over μ_m while increasing both ISR and BC load resulted in the most significant enhancement.

3.2.3. Biodegradability

Table 2 shows the BMP_{Th} for the AcoD of *C. vulgaris* and cellulose at each condition. As previously stated, variable BMP_{Th} is obtained from the mixture of the substrates at the different C/N ratios. The BMP_{Th} at the C/N ratios 7, 16 and 25 corresponded to 571, 477 and 454 mL CH₄/g VS, respectively. The differences in BMP_{Th} in addition to the BMP_{Exp} dramatically affected the BD values, which ranged at 43–66 %. Even though the BMP_{Th} increased when lowering the C/N ratio, the actual BMP and BD values were reduced due to the complexity, recalcitrance, and difficulty to degrade *C. vulgaris* (Bohutskyi et al., 2018). Hence, an inhibitory effect originated principally by reducing ISR, increasing the content of *C. vulgaris*, and in consequence, reducing the C/N ratio could have hindered the BD values.

3.2.4. Fate of inorganic nitrogen

To study the fate of organic nitrogen at the end of AcoD of microalgae and cellulose, both solid and liquid phases were separated and analysed (Table 2). The TAN on the liquid phase was measured by spectrophotometry, while the N-content on the decanted solid was quantified by elemental CHNS analysis. TAN values were considerably low for all experimental conditions (17–30 mg/L), slightly higher with BC addition and at a lower C/N ratio. This behaviour contrasts the reported by Lu et al. (2019) for the AcoD of *Chlorella* sp. with septic tank sludge. They obtained a final TAN of approximately 200–2300 mg/L, although even these levels showed no inhibitory effect over methanogenic activity. The N content of the remaining solids comprised by the digestate and BC was slightly higher at a lower C/N ratio and without BC addition, although the general values were similar to the N content of the inoculum (3.7 %). This behaviour, in addition to the BMP yields and BD, suggests adequate digestion of the microalgae, without ammonia inhibition even at the lowest C/N ratios.

3.2.5. Volatile fatty acids and pH

Fig. 4a exhibit the VFAs accumulated at the end of the AcoD experimental design. The less favourable conditions in terms of lower ISR and C/N resulted in a greater VFA accumulation. Nevertheless, such low concentrations could be considered negligible in all cases. Fig. 4b shows the pH at the beginning and end of the AcoD. No pH adjustment was performed to evaluate the effect of the processing conditions C/N ratio, ISR and BC load. The initial pH (7.5–7.9) was similar for all systems, although higher than the optimal levels for the AD process (pH 6.7–7.4).

Table 2

Average biomethane experimental yield, biodegradability, nitrogen fate and kinetic data for the anaerobic co-digestion of *Chlorella vulgaris* and cellulose obtained for the experimental design.

Independent variables			Experimental				Modified Gompertz			
C/N	ISR	BC load	BMP _{Exp} (mL CH ₄ /g VS)	BD(%)	TAN(mg NH ₃ -N/L)	N (%)	BMP _{max} (mL CH ₄ /g VS)	μ _m (mL CH ₄ /g VS-d)	λ(d)	
7	1	0	270.1	47.3	20.8	4.3	265.9	45.3	0.0	
7	1	3	247.3	43.3	30.3	4.0	242.2	42.8	0.0	
7	2	0	277.6	48.6	17.2	4.0	274.9	59.0	0.0	
7	2	3	259.0	45.3	24.3	4.1	258.6	70.2	0.0	
16	1.5	1.5	275.0	57.7	19.5	3.1	274.0	49.5	0.0	
25	1	0	298.9	65.9	17.2	3.9	294.2	41.8	0.4	
25	1	3	287.5	63.4	22.2	3.0	283.7	44.4	0.1	
25	2	0	295.7	65.2	15.5	3.3	298.5	49.7	0.1	
25	2	3	272.5	60.1	17.1	3.0	270.2	66.2	0.2	

BMP_{Exp} maximum experimental methane yield; BD biodegradability; TAN total ammonia nitrogen measured on the supernatant; N content measured in the decanted solid by ultimate CHNS analysis; BMP_{max} maximum methane yield; μ_m methane production yield; λ duration of lag phase.

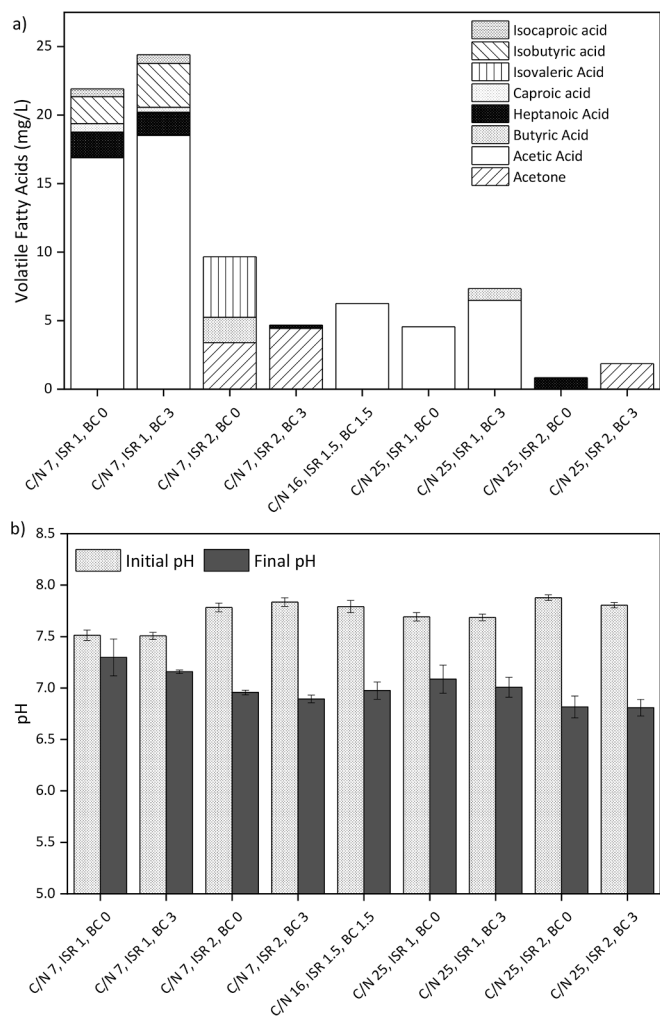


Fig. 4. Anaerobic co-digestion of cellulose and *C. vulgaris* for the factorial design 2³ conditions. a) Accumulated volatile fatty acids accumulated; b) pH.

By the end of the digestion, the systems exhibited different pH variations with final pH of 6.8–7.3, within the optimal range. Increasing ISR and C/N ratio reduced the final pH, with a statistically significant effect ($p < 0.05$). This effect is contrary to the expected since higher ISR and balanced C/N ratios are associated with pH buffering. Even though BC is an alkaline additive and it previously proved to offer a buffering effect on AcoD, under these conditions its addition had no effect on the pH ($p > 0.05$).

3.2.6. Regression model fitting

The parameters BMP_{Exp}, BMP_{max} and μ_m were selected as response variables for the analysis of the factorial design. The regression models obtained were statistically significant with $p < 0.05$ and F-value > F-critical at the 0.05 alpha level (Supplementary data). The centre points included in the 2³-design protected against curvature from second-order effects, validating the fitting of the first-order regression model ($p < 0.05$). Eq. 6, 7 and 8 show the factorial regression models for BMP_{Exp}, BMP_{max} and μ_m. These regressions exhibited R² of 0.73, 0.85 and 0.84, respectively. Hence, only 15–27 % of the variability cannot be explained by the models. The adjusted R² 0.69–0.80 values were fitted to the actual size of the model and the number of factors, whereas the prediction R² 0.58–0.67 indicates the variability that the model would explain during the prediction of new data. In brief, the significance and fitting of the quadratic models to the experimental data were satisfactory.

$$BMP_{Exp} = 275.95 + 12.58 * CN + 0.13 * ISR - 9.53 * BC - 4.69 * CN * ISR \quad (6)$$

$$BMP_{max} = 273.58 + 13.13 * CN + 2.00 * ISR - 9.86 * BC - 4.32 * CN * ISR \quad (7)$$

$$\mu_m = 52.11 + 8.83 * ISR + 3.48 * BC + 3.45 * ISR * BC \quad (8)$$

From the analysis of variance, each factor and interaction of factors offered a specific coefficient and p-value (at 95 % confidence) as listed in Table 3. The significant specific coefficients ($p < 0.05$) for the factors and interactions are part of the regression models. Even though the factor ISR was non-significant for BMP_{Exp} and BMP_{max} (Eq. 6 and 7), the coefficients were kept based on the hierarchy principle. This principle promotes internal consistency by indicating that if a model contains a high order term (CN*ISR), it must contain all the lower order terms (CN and ISR) (Montgomery, 2013). The factors C/N ratio and BC load influenced both BMP_{Exp} and BMP_{max}, with no significant effect from ISR. The C/N ratio did not affect the response variable μ_m, which was influenced exclusively by ISR and BC load and their interaction.

3.2.7. Influence of main factors and interactions

In this experiment, the factor ISR showed no statistically significant differences in BMP_{Exp} and BMP_{max} (Table 3). Moset et al. (2015) reported that regardless of the substrate used, the BMP enhanced as the ISR increased over a range of 1.5–2.5, although not significantly. Similarly, De la Rubia et al. (2018) studied the influence of ISR from different inoculum sources on the AD of the process water obtained from the hydrothermal carbonisation of dewatered sewage sludge. When using sewage sludge inoculum, they observed that the ISR had no significant difference over BMP. These reports agree with the negligent impact of ISR on BMP observed in this experiment. Regardless of the nature and complexity of the substrate used, the BMP was not affected by ISR if an appropriate range is selected (ISR 1.0–2.0).

ISR enhanced the response variable μ_m showing a statistically significant effect. The initial inoculum concentration is reported to influence the rate of substrate hydrolysis. Hence, higher ISR often results in

Table 3
Statistical evaluation of the factors and interactions comprising the factorial regression models.

Coefficient probability							
Term	BMP _{Exp} Coefficient	p-value	BMP _{max} Coefficient	p-value	μ_m Coefficient	p-value	
Constant	275.95	0.000	273.58	0.000	52.11	0.000	
CN	12.58	0.000	13.13	0.000	-1.91	0.080	
ISR	0.13	0.951	2.00	0.246	8.83	0.000	
BC	-9.53	0.000	-9.86	0.000	3.48	0.003	
CN*ISR	-4.69	0.047	-4.32	0.018	-1.42	0.185	
CN*BC	1.69	0.705	0.15	0.927	1.28	0.231	
ISR*BC	-0.95	0.671	-1.30	0.447	3.45	0.003	
CN*ISR*BC	-1.98	0.380	-3.15	0.075	0.02	0.984	

BMP_{Exp} maximum experimental methane yield; BMP_{max} maximum methane yield, μ_m methane production yield.

faster fermentation and consequence enhanced production rate (Raposo et al., 2011). Similarly, Raposo et al., (2009) studied the impact of ISR 0.8–3.0 on the AD of sunflower oil cake. They observed a maximum production rate at ISR 2.0. However, unlike the linear trend observed in this study, they obtained higher μ_m at ISR 2.0 > 1.0 > 3.0 > 0.8 > 1.5 > 0.5.

The impact of microalgae and cellulose addition to varying the C/N ratio showed a significant difference over BMP_{Exp} and BMP_{max} but not over μ_m . The range of C/N ratio selected for this experiment started at an optimal ratio of 25 and moved downward to less favourable conditions. Hence, higher BMP yields were obtained according to the following C/N ratio order 25 > 16 > 7. Similarly, Bohutskyi et al. (2018) observed a synergistic effect by co-digesting algae and cellulose. They reported the highest BMP yields and production rate at C/N ratios of 21 and 34 than lower ratios or even the mono-digestion of each substrate. Therefore, increasing the C/N ratio enhanced BMP yields but did not influence the production rate.

BC load had a statistically significant effect on all variables ($p < 0.05$). For BMP yield, the coefficient of BC load had a negative value, which indicates that increasing the BC load would result in lower BMP. This response contrasts to the observed in the previous section, where BC drastically enhanced BMP yields at ISR 0.5–0.9 and C/N ratio 10–30. On the other hand, increasing BC load led to higher μ_m which partially agrees with previous experiments with the addition of this same oak wood BC. The addition of BC at a load of 3 % during the AD of cellulose slightly enhanced BMP yields (7 %), whereas it doubled μ_m (Quintana-Najera et al., 2021). Reports of BC addition during the AD of microalgae demonstrated the importance of BC load. Deng et al. (2020) studied the AD of *Laminaria digitata* and *Saccharina latissima* at variable BC loads. For *L. digitata*, a BC addition of 0.06 and 0.125 % enhanced BMP yields and μ_m , whereas higher BC loads of 0.5 and 1.0 % reduced both parameters. Conversely, for the AD of *S. latissima* BC loads < 0.5 % had no significant influence, whereas BC load of 0.5 and 1.0 enhanced both BMP and μ_m . The latter suggests that BC load influenced BMP yields and production rate, but the effect level was subjected to the substrate employed. Therefore, it is necessary to establish the optimum BC load for achieving the highest BMP yield and productivity for each potential substrate.

3.2.8. Optimisation of biomethane

Graphical interpretation of the responses facilitates the examination of factors and interactions in regression models. Contour plots with a combination of the three factors C/N, ISR and BC were used for visualising the optimum areas for each response variable (Fig. 5). As expected, the contour plots for BMP_{Exp} and BMP_{max} are similar. The stretching of the axis indicates that maximum values can be obtained at C/N 22–25 and BC 0–1.5 regardless of the ISR. The contour plots for μ_m differed since maximum values were obtained at ISR of 1.7–2.0 and BC load of 1–3, regardless of the C/N ratio. The interaction plots for BMP showed that the C/N ratio played a major role (Fig. 5a and b). This factor also interacted strongly with the rest, indicating a predominant

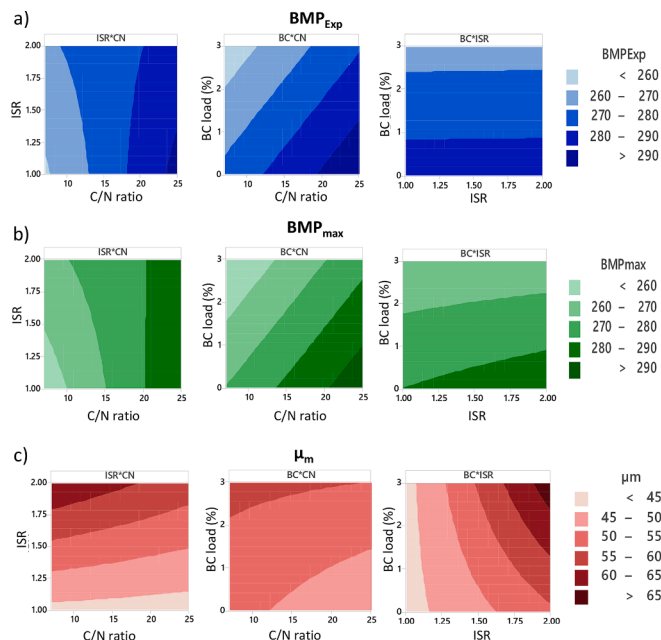


Fig. 5. Contour plots for interaction effects and optimised area obtained by response surface regression. a) Experimental methane yield (BMP_{Exp}); b) maximum methane yield (BMP_{max}); c) methane production rate (μ_m).

influence. In the case of μ_m , ISR exhibited the major effect, while its interaction with BC load was significant on the response in agreement to the regression models (Fig. 5c).

The response variables BMP_{Exp}, BMP_{max} and μ_m were analysed by the D function for the factorial regression optimisation. The objective was to improve these parameters to achieve maximum suitability. Composite D assessed how the combined variables satisfy the response. Hence, the optimum conditions obtained were C/N 25, ISR 2.0 and BC load 0.58 % with the highest possible BMP of 294 mL CH₄/g VS, and μ_m of 57 mL CH₄/g VS-d. A D-value of 0.62 indicated that all responses were predicted to be within the desired limits. A further AcoD experiment under these optimal conditions is shown as supplementary data. The obtained final BMP (312 mL CH₄/g VS-d) was even higher than the predicted, supporting the relevance of the model.

Response optimisation for obtaining maximum biomethane allowed the prediction and evaluation at other C/N ratios. For instance, as the C/N ratio is reduced to 16 and 7, the optimum ISR must be maintained at 2, while BC load decreased at 0.34 and 0 %, respectively. These experimental conditions will result in BMP yields of 284 and 275 mL CH₄/g VS and μ_m of 55.6 and 54.0 mL CH₄/g VS-d, respectively. Regression model and response optimisation proved to be useful when working with variable C/N ratios due to variability in substrate composition and availability.

4. Conclusions

This study demonstrated the importance of the C/N ratio, ISR and BC load during the anaerobic co-digestion of *C. vulgaris* and cellulose. ISR 0.5–0.9 exhibited low BMP yields, which were considerably improved by BC addition that also provided a pH buffering effect. Regression models and optimisation analysis demonstrated that as the C/N ratio is reduced, the BC load should also be reduced to achieve better performance. Hence, the beneficial effect of BC addition was more visible at higher C/N ratios, suggesting that the BC effect is highly dependent on the digestion conditions.

CRedit authorship contribution statement

Jessica Quintana-Najera: Conceptualization, Investigation, Data curation, Formal analysis, Methodology, Project administration, Resources, Software, Validation, Visualization, Writing – original draft, Writing – review & editing. **A. John Blacker:** Conceptualization, Investigation, Project administration, Resources, Supervision. **Louise A. Fletcher:** Conceptualization, Investigation, Supervision. **Andrew B. Ross:** Conceptualization, Funding acquisition, Investigation, Project administration, Resources, Supervision, Validation, Visualization, Writing – review & editing.

Declaration of Competing Interest

The authors declare that they have no known competing financial interests or personal relationships that could have influenced the work reported in this paper.

Acknowledgements

This research was funded by CONACYT-SENER, Autonomous University of Sinaloa and the Biotechnology and Biological Sciences Research Council (BBSRC) through BEFWAM project [grant BB/S011439/1]. The authors would also like to acknowledge Esholt Wastewater Treatment Plant for providing inoculum samples.

Appendix A. Supplementary data

Supplementary data to this article can be found online at <https://doi.org/10.1016/j.biortech.2021.126086>.

References

- APHA, 2005. Standard methods for the examination of water and wastewater. Washington DC, USA.
- Aragón-Briceño, C.I., Grasham, O., Ross, A.B., Dupont, V., Camargo-Valero, M.A., 2020. Hydrothermal carbonization of sewage digestate at wastewater treatment works: Influence of solid loading on characteristics of hydrochar, process water and plant energetics. *Renew. Energy* 157, 959–973. <https://doi.org/10.1016/j.renene.2020.05.021>.
- Bohutskiy, P., Phan, D., Kopachevsky, A.M., Chow, S., Bouwer, E.J., Betenbaugh, M.J., 2018. Synergistic co-digestion of wastewater grown algae-bacteria polyculture biomass and cellulose to optimize carbon-to-nitrogen ratio and application of kinetic models to predict anaerobic digestion energy balance. *Bioresour. Technol.* 269, 210–220. <https://doi.org/10.1016/j.biortech.2018.08.085>.
- Buswell, A.M., Mueller, H.F., 1952. Mechanism of Methane Fermentation. *Ind. Eng. Chem.* 44 (3), 550–552.
- Chronakis, I.S., Madsen, M., 2011. Algal proteins. *Handbook of Food Proteins*. Woodhead Publishing 353–394.
- De la Rubia, M.A., Villamil, J.A., Rodriguez, J.J., Mohedano, A.F., 2018. Effect of inoculum source and initial concentration on the anaerobic digestion of the liquid fraction from hydrothermal carbonisation of sewage sludge. *Renew. Energy* 127, 697–704. <https://doi.org/10.1016/j.renene.2018.05.002>.
- Deng, C., Lin, R., Kang, X., Wu, B., O'Shea, R., Murphy, J.D., 2020. Improving gaseous biofuel yield from seaweed through a cascading circular bioenergy system integrating anaerobic digestion and pyrolysis. *Renew. Sustain. Energy Rev.* 128, 109895. <https://doi.org/10.1016/j.rser.2020.109895>.
- IEA, 2020. Outlook for biogas and biomethane. International Energy Agency.
- Klüpfel, L., Keilweil, M., Kleber, M., Sander, M., 2014. Redox properties of plant biomass-derived black carbon (biochar). *Environ. Sci. Technol.* 48, 5601–5611. <https://doi.org/10.1021/es500906d>.
- Lee, J., Kim, K.H., Kwon, E.E., 2017. Biochar as a Catalyst. *Renew. Sustain. Energy Rev.* 77, 70–79. <https://doi.org/10.1016/j.rser.2017.04.002>.
- Li, R., Duan, N., Zhang, Y., Liu, Z., Li, B., Zhang, D., Dong, T., 2017. Anaerobic co-digestion of chicken manure and microalgae *Chlorella* sp.: Methane potential, microbial diversity and synergistic impact evaluation. *Waste Manag.* 68, 120–127. <https://doi.org/10.1016/j.wasman.2017.06.028>.
- Lu, D., Liu, X., Apul, O.G., Zhang, L., Ryan, D.K., Zhang, X., 2019. Optimization of biomethane production from anaerobic Co-digestion of microalgae and septic tank sludge. *Biomass Bioenergy* 127, 105266. <https://doi.org/10.1016/j.biombioe.2019.105266>.
- Mata-Alvarez, J., Dosta, J., Macé, S., Astals, S., 2011. Codigestion of solid wastes: A review of its uses and perspectives including modeling. *Crit. Rev. Biotechnol.* 31 (2), 99–111. <https://doi.org/10.3109/07388551.2010.525496>.
- Montgomery, D.C., 2013. Design and analysis of experiments, Eight Edit. ed. John Wiley & Sons, Inc.
- Moset, V., Al-zohairi, N., Møller, H.B., 2015. The impact of inoculum source, inoculum to substrate ratio and sample preservation on methane potential from different substrates. *Biomass and Bioenergy* 83, 474–482. <https://doi.org/10.1016/j.biombioe.2015.10.018>.
- Mumme, J., Srocke, F., Heeg, K., Werner, M., 2014. Use of biochars in anaerobic digestion. *Bioresour. Technol.* 164, 189–197. <https://doi.org/10.1016/j.biortech.2014.05.008>.
- Okoro-Shekwa, C.K., Turnell Suruagy, M.V., Ross, A.B., Camargo-Valero, M.A., 2020. Particle size, inoculum-to-substrate ratio and nutrient media effects on biomethane yield from food waste. *Renew. Energy* 151, 311–321. <https://doi.org/10.1016/j.renene.2019.11.028>.
- Paritosh, K., Vivekanand, V., 2019. Biochar enabled syntrophic action: Solid state anaerobic digestion of agricultural stubble for enhanced methane production. *Bioresour. Technol.* 289, 121712. <https://doi.org/10.1016/j.biortech.2019.121712>.
- Piątek, M., Lisowski, A., Kasprzycka, A., Lisowska, B., 2016. The dynamics of an anaerobic digestion of crop substrates with an unfavourable carbon to nitrogen ratio. *Bioresour. Technol.* 216, 607–612. <https://doi.org/10.1016/j.biortech.2016.05.122>.
- Quintana-Najera, J., Blacker, A.J., Fletcher, L.A., Ross, A.B., 2021. The effect of augmentation of biochar and hydrochar in anaerobic digestion of a model substrate. *Bioresour. Technol.* 321, 124494. <https://doi.org/10.1016/j.biortech.2020.124494>.
- Raposo, F., Borja, R., Martín, M.A., Martín, A., de la Rubia, M.A., Rincón, B., 2009. Influence of inoculum-substrate ratio on the anaerobic digestion of sunflower oil cake in batch mode: Process stability and kinetic evaluation. *Chem. Eng. J.* 149 (1–3), 70–77. <https://doi.org/10.1016/j.cej.2008.10.001>.
- Raposo, F., Fernández-Cegri, V., De la Rubia, M.A., Borja, R., Béline, F., Cavinato, C., Demirer, G., Fernández, B., Fernández-Polanco, M., Frigon, J.C., Ganesh, R., Kapparaju, P., Koubova, J., Méndez, R., Menin, G., Peene, A., Scherer, P., Torrijos, M., Uellendahl, H., Wierinck, L., de Wilde, V., 2011. Biochemical methane potential (BMP) of solid organic substrates: Evaluation of anaerobic biodegradability using data from an international interlaboratory study. *J. Chem. Technol. Biotechnol.* 86 (8), 1088–1098. <https://doi.org/10.1002/jctb.2622>.
- Shanmugam, S.R., Adhikari, S., Nam, H., Kar Sajib, S., 2018. Effect of bio-char on methane generation from glucose and aqueous phase of algae liquefaction using mixed anaerobic cultures. *Biomass and Bioenergy* 108, 479–486. <https://doi.org/10.1016/j.biombioe.2017.10.034>.
- Sterling, M.C., Lacey, R.E., Engler, C.R., Ricke, S.C., 2001. Effects of ammonia nitrogen on H₂ and CH₄ production during anaerobic digestion of dairy cattle manure. *Bioresour. Technol.* 77 (1), 9–18. [https://doi.org/10.1016/S0960-8524\(00\)00138-3](https://doi.org/10.1016/S0960-8524(00)00138-3).
- Wang, G., Li, Q., Gao, X., Wang, X.C., 2018. Synergetic promotion of syntrophic methane production from anaerobic digestion of complex organic wastes by biochar: Performance and associated mechanisms. *Bioresour. Technol.* 250, 812–820. <https://doi.org/10.1016/j.biortech.2017.12.004>.
- Wang, M., Sahu, A.K., Rusten, B., Park, C., 2013. Anaerobic co-digestion of microalgae *Chlorella* sp. and waste activated sludge. *Bioresour. Technol.* 142, 585–590. <https://doi.org/10.1016/j.biortech.2013.05.096>.
- Ward, A.J., Lewis, D.M., Green, F.B., 2014. Anaerobic digestion of algae biomass: A review. *Algal Res.* 5, 204–214. <https://doi.org/10.1016/j.algal.2014.02.001>.
- Xiao, K.K., Guo, C.H., Zhou, Y., Maspolim, Y., Wang, J.Y., Ng, W.J., 2013. Acetic acid inhibition on methanogens in a two-phase anaerobic process. *Biochem. Eng. J.* 75, 1–7. <https://doi.org/10.1016/j.bej.2013.03.011>.
- Yao, Y., Zhang, R., Wang, B., Zhang, S., 2017. Modeling and optimization of anaerobic digestion of corn stover on biogas production: Initial pH and carbon to nitrogen ratio. *Energy Sources. Part A Recover. Util. Environ. Eff.* 39 (14), 1497–1503. <https://doi.org/10.1080/15567036.2017.1336821>.
- Yen, H.W., Brune, D.E., 2007. Anaerobic co-digestion of algal sludge and waste paper to produce methane. *Bioresour. Technol.* 98 (1), 130–134. <https://doi.org/10.1016/j.biortech.2005.11.010>.
- Zhang, Y., Caldwell, G.S., Zealand, A.M., Sallis, P.J., 2019. Anaerobic co-digestion of microalgae *Chlorella vulgaris* and potato processing waste: Effect of mixing ratio, waste type and substrate to inoculum ratio. *Biochem. Eng. J.* 143, 91–100. <https://doi.org/10.1016/j.bej.2018.12.021>.
- Zhao, Z., Zhang, Y., Woodard, T.L., Nevin, K.P., Lovley, D.R., 2015. Enhancing syntrophic metabolism in up-flow anaerobic sludge blanket reactors with conductive carbon materials. *Bioresour. Technol.* 191, 140–145. <https://doi.org/10.1016/j.biortech.2015.05.007>.
- Zwietering, M.H., Jongenburger, I., Rombouts, F.M., Van 'T Riet, K., 1990. Modeling of the Bacterial Growth Curve. *Appl. Environ. Microbiol.* 1875–1881.